The role of organics in relation to corrosion in steam-water systems

Yu Xue[1,7], Karlien Dejaeger[1,7], Ben Bischoff Tulleken[2], Duygu Disci[3], Peter Janssen[4], Andrea M Brunner[5], David Moed[6], Wolfgang Hater[3], Emile R Cornelissen[1,5,7], Marjolein Vanoppen[1,7]

[1] Particle and Interfacial Technology Group (PaInT), Department of Green Chemistry and Technology, Faculty of Bioscience Engineering, Ghent University, Coupure Links 653, 9000 Ghent, Belgium

[2] CITG, Section Sanitary Engineering, Department of Water Management, Faculty of Civil Engineering and Geosciences, Delft, Stevinweg 1, 2628 CN, Delft, the Netherlands

[3] Kurita Europe GmbH, Theodor-Heuss-Anlage 2, 68165 Mannheim, Germany

[4] Sitech Services, Urmonderbaan 22, 6167 RD Geleen, The Netherlands

[5] KWR Water Research Institute, PO box 1072, 3430 BB, Nieuwegein, The Netherlands

[6] Evides Industriewater, PO Box 4472, 3006 AL Rotterdam, the Netherlands

[7] Centre for Advanced Process Technology for Urban REsource recovery (CAPTURE), Frieda Saeysstraat, 9052 Ghent, Belgium

Abstract

A sampling campaign was conducted in a film-forming amine product (FFAP)-treated high pressure steam-water system of an ammonia producing plant to optimize the cycle chemistry. The IAPWS and VGB guidelines were assessed to be applicable with modifications fitting the local situation according to the pH and conductivity. Methanol, a main organic compound originating from the production process, entered the steam-water system with the process condensate and was tested possible to degrade into formate, which is a known low molecular weight degradation product. Furthermore, organic compounds from cation exchange resin were found in blowdown streams, suspected to originate from resin carryover. No operational and corrosion issues were observed.

Lab-scale first condensate experiments confirmed that a lower pH was present in the first condensate compared with the bulk steam, however, it was still partially buffered by ammonia. Via corrosion tests it was observed that Oleylpropylendiamine (OLDA), in addition to ammonia, formed a smoother and more uniform magnetite layer. Moreover, magnetite layers formed under OLDA added to ammonia were more resistant against acidic conditions (pertinent to condensate return systems) than layers formed under the ammonia only chemistry, and blank chemistry (without a chemical additive), with less reduction of the magnetite layer thickness.

These studies in combination with the plant experiences confirm that the steam-water system can be safely run with the selected FFAP treatment concept even with organics from the production process.

Key words

Film-forming amine; Steam-water system; Organic compounds; First condensate.

1 Introduction

Steam is important in the (petro)chemical industry, where it is used for heat transfer, as a reaction medium, and even for direct contact with crude feed in steam crackers. Return of steam condensates as boiler feed water reduces both water and energy consumption [1]. On the other hand, efficient steam production and conditioning is a major factor influencing water and energy use within the (petro)chemical industry, where the prevention of corrosion and fouling has a substantial influence on the efficiency of heat transfer.

Corrosion is considered a major factor in the performance of steam-water cycles (SWC). Magnetite ($Fe^{3+}{}_2Fe^{2+}O_4$) is the most common corrosion product (oxide layer) formed in the SWC, when all-volatile treatment with reducing conditions (AVT-R) is applied. This iron-oxide is formed via a two-step reaction, the formation of ferrous iron followed by the Schikorr reaction [2]. This reaction forms an oxide-layer in two directions, as a dense and protective layer into the steel surface, and a porous top layer on the steel surface.

Film forming substances are being utilized worldwide as means to mitigate corrosion during plant operation and during plant shutdown/layup. Film forming amines (FFAs) are the most commonly used type of corrosion inhibitor. They consist of primary and/or secondary amine groups with a saturated or unsaturated aliphatic carbon chain [3]. They form a protective (hydrophobic) film on the inner (metal) surface of the steam-water system to create a barrier between the metal surface and the stream. A well-known and thoroughly studied type of FFA is oleyl propylenediamine (OLDA). Commercial film forming amine products (FFAPs) are applied as emulsion in water which may contain other substances, such as alkalizing amines, emulsifiers, reducing agents and dispersants[3,4]. They show the necessary long term storage stability and shelf life. Moreover, the combinations of FFAs and alkalizing amines result in a smooth and compact magnetite layer with better resistant to further corrosion [5–8]. The corrosion inhibiting effect of FFAs and FFAPs have been studied in lab and field conditions, where a decrease in corrosion rates and FAC was reported [5,6,8–12].

Despite their promising protection towards corrosion, several investigations have shown that FFAP can degrade into low molecular weight organic acids, like formate and acetate, in steam-water cycles due to hydrothermolysis [13–15]. Furthermore, there are other organic compounds in the SWC, including natural organic matter, process contaminants and contaminants from other sources possibly breaking down into organic acids as well. It was reported that the concentration of methanol, one of the main process contaminants from an ammonia plant, can be 13-18 mg/L in the boiler feed water [16]. It entered the SWC through the process condensate. The degradation of methanol is thus interesting regarding the formation of organic acids. pH and conductivities (direct conductivity, conductivity after

cation exchanger and degassed conductivity after cation exchanger) are the key parameters to monitor the cycle chemistry in SWC. The International Association for the Properties of Water and Steam (IAPWS) released a technical guidance document on the volatile treatments, in which only volatile alkalizing agents are used, for the steam-water circuits of fossil and combined cycle/HRSG power plants in 2015 [17]. It set guidelines for pH, conductivities, as well as for dissolved oxygen, sodium and SiO_2 in different units from various types of system. This guideline was suggested for pH control in film-forming substance (including FFA)-treated steam-water systems [3]. There is also a guideline from VGB PowerTech e.V. (VGB), published in 2011, providing chemical specification for different types of steam-water systems to ensure the water/steam quality [18]. Not meeting the specifications defined in these guidelines is generally considered an increased risk for the occurrence of corrosion in the SWC.

Apart from the pH guidelines for bulk steam/water streams, there is a general concern that formate and acetate, as known degradation products from organic matter, cause a local pH drop in the first condensate area. Here, the steam is condensed to the first initial water droplets which is mostly due to a pressure drop [19]. An early condensate sampler has been used in the past to mimic this first condensate and study its risk for corrosion [20–22]. In this case, superheated steam is extracted from an industrial steam system and is subsequently cooled down by a heat exchanger and analyzed. However, this is not really the first liquid phase [20]. Furthermore, the additional protection that FFA could provide against FAC in the zone of the first condensate has not yet been investigated.

The Steam and Condensate Quality Water Process Technology project [23] tackled the above mentioned problems. It was established by Dow Benelux B.V. Terneuzen, Evides Industriewater, Sitech Services, KWR Water Research Institute, Ghent University, Kurita Europe GmbH, and the Institute for Sustainable Process Technology (ISPT). ISPT, located in the Netherlands, is an independent party which supports developing technologies and act as driver for the sustainability transition, especially on process technology [24]. The main goal of this project were

- to enable a reduction in energy and water consumption by gaining more insight in conditioning and treatment of steam condensates (reported elsewhere [25,26])
- to establish a clear understanding and well-founded view on the (corrosion) risks related to boiler feed water that is not reaching the required feed water quality specifications defined by major guidelines [17,18] (mainly with regards to the presence of organic contaminants).

The latter objective will be the focus of this paper.

Sampling work was performed in a steam-water system in an ammonia plant located in Geleen, the Netherlands. It has a daily NH_3 production of 1600t. Due to several boiler tube failures caused by phosphate corrosion under heavy local magnetite deposition, the boiler water treatment program was

switched in 2013 from the combination of hydrazine, trisodium phosphate and ammonia to the combination of Cetamine®, an OLDA-based FFAP, and Ferrolix®, a product containing an alkalizing amine. With the new treatment, no more boiler tube failures occurred [27]. It was reported about one year after the FFAP treatment that lumps of resin beads were detected in the turbine condensate mixed bed during the separation phase of the regeneration cycle. Meanwhile, there was an increase in the frequency of regenerations. The resin beads were found partially mechanically broken due to aging and fouled by iron and organics. After cleaning and partial replacement of the resin beads, the problem did not occur anymore. In fact, the cleaning effect (removal of iron-oxides/phosphate deposits) observed with FFAP treatment, especially in the initial phase of the treatment, is well known and the application can be easily adapted accordingly. However, the unfortunate mechanical breakage of the resin beads led to the malfunctioning. This example still illustrates the necessity of careful monitoring of the additives and organics. To assess organic breakdown product formation, a screening protocol was developed using liquid chromatography coupled to the high-resolution mass spectrometry (LC – HRMS) in earlier work within this project [28]. This screening protocol is also applicable for the study of organic compounds, for example breakdown products from the floating resin.

The objectives of this paper are

- investigating the distribution of organic compounds originating from the full-scale steam-water system and the thermal stability of methanol, as a process contaminant, with a lab-scale boiler set-up
- designing a lab-scale set-up to simulate and study the first condensate in a controlled way, and
- studying corrosion under dynamic conditions with the pH of the first condensate and the additional protection of FFAs.

2 Experimental

2.1 Sampling campaign in a full-scale steam-water system

A sampling campaign was conducted in an FFAP-treated full-scale high pressure (HP) steam-water system to investigate the organic compounds and their distributions in the system. There were 14 sampling points selected from the feed water section, steam drums and turbine and process condensate streams (Figure 1, and Table 1 with temperatures and pressures). pH was measured on-site prior to taking samples from each sampling point. After the pH measurements, samples were taken for conductivity and LC—HRMS analyses. The details of the LC—HRMS method and the data analysis method were reported by Xue *et al*. (2020) [28]. All samples were collected on the same day and were sent to the analytical labs within 24 hours after the campaign.

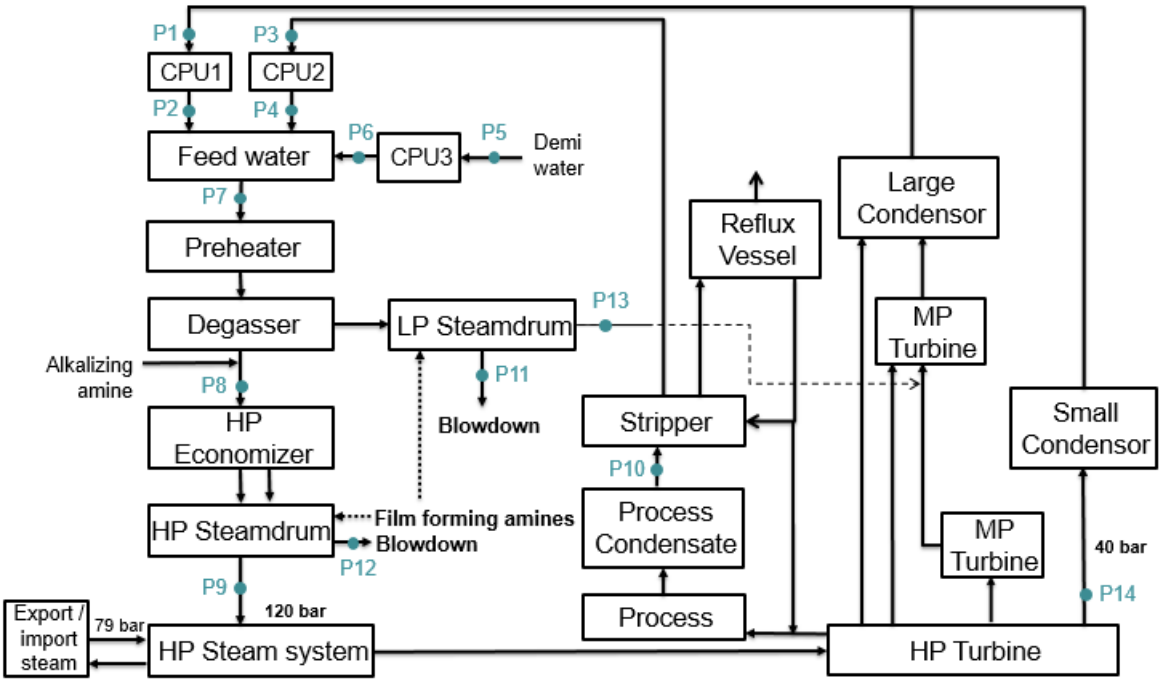

Figure 1. Schematic of the steam-water system showing the sampling points (P1 – P14), CPU = condensate polishing unit, LP = low pressure, MP = medium pressure, HP = high pressure.

Table 1. Temperature and pressure conditions of the 14 sampling points.

Sampling point	T (°C)	P (bar)
1	40	4
2	40	4
3	60	4
4	60	4
5	20	4.5
6	20	4.5
7	60	5
8	130-230	120
9	520	120
10	30	Unknown
11	~ 135	3
12	330	120
13	~ 135	4.5
14	405	40

2.2 Lab-scale boiler experiments

Methanol was reported as a major TOC contributor in this steam-water system [16]. Two lab-scale boiler experiments were performed to study the effect of pH on the methanol stability (Figure 2A). The feed solution contained 13 mg/L methanol in both experiments 1 and 2, which was the reported methanol concentration in the plant [16]. In experiment 2, ammonia (NH_4OH) was added to the feed solution as well until pH 8.9 was reached, similar to the alkalized environment in the full-scale system. The mini-boiler, tubing and connections were all made of stainless steel. The conditions of HP steam system were chosen for these experiments. The HPLC pump (LabAlliance series II, US) was set to 2.0 mL/min to achieve a residence time of 6 s, mimicking the residence time of steam in the HP steam system in the full-scale plant. The temperature of the fluidized sand bath (FSB-3, Omega, US), in which the mini-boiler was submerged, was set to 520°C, regulated by a 4838 Parr temperature controller (Parr Instrument Company, US). The temperature feedback was provided by a thermocouple. The fine aluminum oxide particles in the sand bath were fluidized by ambient air. The BPR-valve (back pressure valve) was adjusted to 120 bar, similar to the HP steam system conditions. Samples were taken from the feed bottle and the condensate side in each experiment. The pH of the collected samples were measured (Orion 8107UWMMD electrode with an Orion Star A121 Portable pH Meter, Thermo Fisher Scientific, USA). The samples were also analyzed by gas chromatography-mass spectrometry for methanol and ion chromatography for formate.

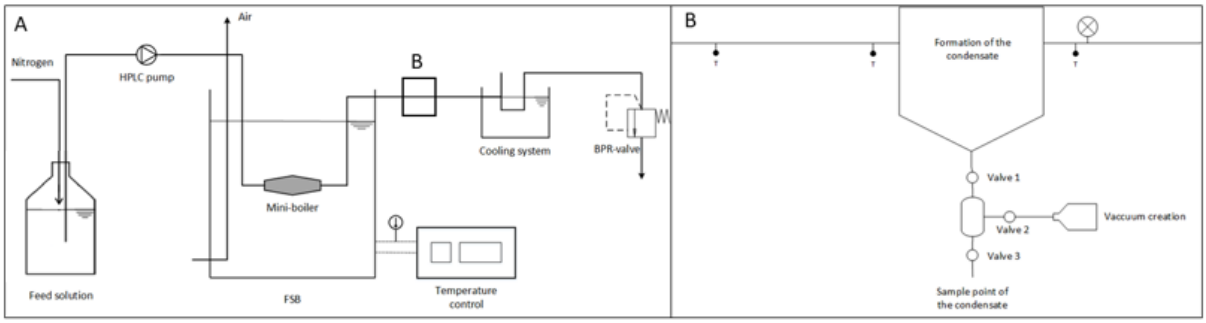

Figure 2. (A) Schematic of the lab-scale boiler setup. HPLC = high-performance liquid chromatography, FSB = fluidized sand bath, BPR-valve = back pressure valve. (B) Extension of the boiler setup for first condensate experiments. The BPR-valve is not used. Mini-boiler is replaced by coiled tubes. T = temperature sensor.

2.2.1 Gas chromatography-mass spectrometry method

A methanol analysis method was developed on a GC-MS (Agilent, USA) with direct liquid injection for a sufficient methanol signal. The injection volume was 1 µL. The split ratio was 35:1. A ZB-5MS Plus column (Phenomenex, California, USA) was used. The column oven program was 45°C to 150°C with a ramp of 30°C/min. The flow rate was 1.2 mL/min. The methanol samples were stored in 15 mL falcon tubes.

2.2.2 Ion chromatography method

A 930 Compact IC Flex (Metrohm, Herisau, Switzerland) with an IC conductivity detector (Metrohm) was used for the analysis of the small organic acids. A Metrosep A Supp 16 – 250/4.0 anion column (250 mm x 4.0 mm x 4.5 µm, Metrohm) was selected together with a Metrosep A Supp 16 Guard/4.0 as a pre-column. The eluent was 7.5 mM Na_2CO_3 and 0.75 mM NaOH in ultra-pure water. The regenerant comprised 0.2 M oxalic acid, 500 mM H_2SO_4 and 10 % (v/v) acetone. The flow rate of eluent was 0.8 mL/min. The pressure was 14 MPa and the column oven was set to 45°C. The injection volume was 50 µL. Each run lasted 35.4 min.

2.3 First condensate experiments

The lab-scale boiler setup was extended to mimic the homogeneous first condensate in a steam turbine (Figure 2A+B). The entire set-up connection was made from stainless steel 316 tubing (Swagelok, US). The HPLC pump was finally set to a flowrate of 12 mL/min (see results in 3.3.1.). Heat transfer to the tube (replacing the mini-boiler in Figure 2A) was accomplished by the FSB. The FSB-3 temperature was finally set to 250°C (see results). A first condensate chamber (NLT pivaco group, Belgium) was placed after the FSB. The chamber was externally heated with tracing cables and insulated to prevent heat loss (Heattracer, Belgium). The temperature of the steam was measured with three temperature sensors (Jumo Delos T, Germany) before and after the first condensate chamber. The pressure was monitored just after the chamber with a manometer (Swagelok). Bulk steam was cooled at the end by submerging the stainless steel tubing in water at room temperature. The flowrate

of the bulk steam condensate (BC) was measured by logging the cumulative weight in time. First condensate (FC) droplets were collected in the first condensate chamber with a demister and intercepted at the bottom by using an intermediate buffer cylinder and 3 valves (Figure 2B). First, valve 2 was opened to create a vacuum in the small buffer cylinder. Next, valve 2 was closed and valve 1 was opened, pulling the first condensate in the cylinder with a volume of 12.5 mL. Valve 1 was closed and valve 2 and 3 were opened to push the first condensate out the cylinder in a glass vessel. BC was collected with 15 minute time intervals, and 25 mL of first condensate was collected at minute 15 to nearly completely remove all FC liquid from the chamber by filling the buffer cylinder twice.

Two experiments were conducted with a 0.5 mg/L ammonia solution and a 0.5 mg/L solution of ammonia, acetic acid and formic acid. pH, conductivity and ion concentrations were measured for both first condensate, bulk condensate and feed solution (see 2.2). The results were validated with a model, which predicts liquid film pH at a certain temperature and steam quality. The model was reported elsewhere [29], but adjustments were made to extend it to the conditions from this set-up. The adjusted model calculates the pH and relative volatility at room temperature with the assumption that CO_2 from the air dissolves in the samples during sampling.

2.4 Corrosion tests

Corrosion tests were carried out to corroborate the differences of magnetite layers with and without OLDA and the effect of dynamic corrosive medium on these layers using the pH of the first condensate from the previous experiment.

2.4.1 Coupons

Carbon steel grade 1010 coupons with glass beaded finish were used for the corrosion tests. The coupons dimensions are approx. 75x10x1.6 mm. Coupons were delivered and kept in volatile corrosion inhibitor (VCI) filled plastic packaging until the tests. The chemical composition of the carbon steel is provided in Table 2. Prior to immersion tests (see 2.4.3 and 2.4.4), the coupons were removed from the plastic packaging, the length, width, and thickness were measured using a Vernier caliper to the nearest 0.01 mm, and weighed to the nearest 0.1 mg. Afterwards, they were flushed and cleaned with acetone, and dried in air.

Table 2: Chemical composition of the C1010 alloy (wt%).

C	Mn	P	S	Si	Cu	Ni
0.0820	0.4100	0.0120	0.0080	0.0160	0.0580	0.0190
Cr	Mo	Al	V	Ti	N	B
0.0490	0.0080	0.0390	0.0010	0.0020	0.0034	0.000

2.4.2 OLDA stock solution preparation

1 w/w% OLDA and ultrapure water were used to prepare a 500 mg/L solution. After 15 minutes of stirring, a 50 mg/L OLDA solution was made which was immediately diluted to 10 mg/L. The 10 mg/L solution was used to saturate the surface of a flask with OLDA for 24 hours, while the 500 mg/L was kept on the mixing plate. As the 50 mg/L solution was directly consumed after the preparation, clean volumetric flasks were used. The following day the steps were repeated to obtain the desired 10 mg/L OLDA solution in a pre-saturated flask. The prepared solution remained permanently stirred. Analytical control of the solution, using COD measurements, proved a concentration of 10 ± 1 mg/L. Prior to experiment this solution was further diluted to obtain a concentration of 2.5 mg/L.

Bengal Rosa dye combined with acetic acid, and a UV-Vis spectrophotometer were used to construct absorbance-concentration curves as means to determine the FFA concentration after the experiments [30].

2.4.3 Immersion and re-immersion corrosion test setup

The setup for the corrosion tests (Figure 3) was first used for the immersion corrosion test to form the magnetite layer and subsequently for the re-immersion acid tests to measure the stability of the magnetite layer formed in the first part of the test. Coupons were fully submerged into the test solution. Thus, there were only liquid phase interactions without steam influence. The setup consisted of a high temperature, high pressure autoclave lined with PTFE (Berghof BR500, Germany) containing the test solution, heater, temperature controller, thermocouple (Berghof BTC3000), nitrogen purging and pressurizing gas. The custom-made PTFE cylindrical shaped coupon holder contained holes for the coupons to fit in. For the magnetite layer formation immersion corrosion tests, a high-pressure pump (Gilson 305 Master pump, US) with a pressure regulating manometric module was used to add the ammonia (NH_4OH) to the test solution after it has been sparged by nitrogen. This was to avoid ammonia stripping. A balance was used to verify the ammonia addition. The dissolved oxygen level was verified by sparging tests, ranging from 35 to 40 ppb. For the re-immersion tests performed at acidic conditions, the overhead stirrer (Berghof BRM1) was used to generate fluid flow conditions. Ammonia was used to alter the pH, instead of using conventional organic alkalizing amines in FFAP. This was done to avoid any implication by possible decomposition of the alkalizing amines. Since there was only one phase the type of alkalizer is not important.

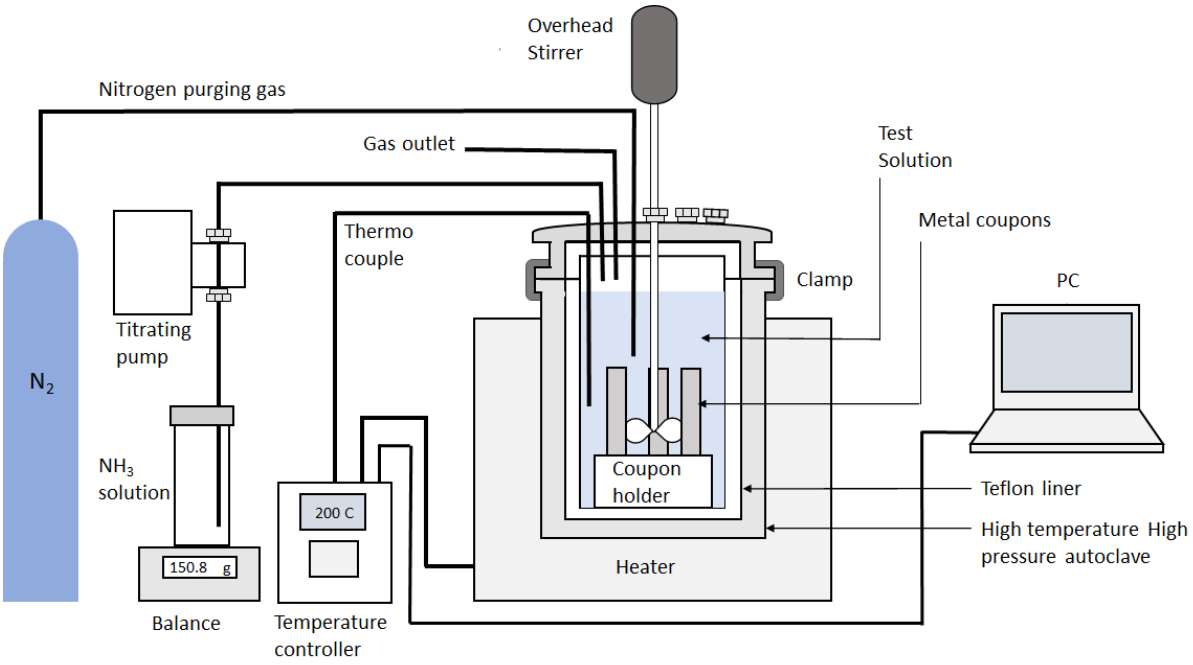

Figure 3. Schematic representation of the test setup for the immersion and re-immersion corrosion experiments.

2.4.4 Test solutions and conditions

A total of three immersion corrosion tests (with a duration of 48h per test) were performed, to evaluate three different chemistries on the formation of a magnetite layer on the C1010 coupons. Four coupons were used per immersion corrosion test, two of them were used for oxide analysis afterwards, and two were used for the re-immersion corrosion test. Meaning, a total of three re-immersion tests (48h) were performed as well. The higher temperature and stagnant conditions during the immersion tests were chosen to promote the magnetite film growth. The re-immersion tests simulated flow conditions under an acidic pH environment. The pH values were decided based on the result of the first condensate experiments (3.3.2). Table 3 provides an overview of the test solutions and conditions used. Runs 1 to 3 mark the different initial test solutions, X.1 stands for an immersion test, and X.2 for a re-immersion test.

Table 3. Overview of the test conditions in immersion and re-immersion experiments.

Experiment		Chemistry condition		Temp	rpm	Velocity	Shear
		Chemical (mg/L)	pH	(°C)	(-)	(m/s)	stress[e] (mPa)
Run 1	Run 1.1	Blank chemistry/ untreated (neutral)	6.5	250 ± 5	0	0	0
	Run 1.2	Acetic acid: 0.08	6.0	150 ± 3	1000	1.9[c] 0.5 - 0.7[d]	178
Run 2	Run 2.1	Ammonia: to pH ca. 9.2 OLDA: 2.44[a]	9.12 ± 0.02[b]	230 ± 2	0	0	0
	Run 2.2	Acetic acid: 0.08	6.1	150 ± 3	1000	1.9[c] 0.5 - 0.7[d]	178
Run 3	Run 3.1	Ammonia: to pH ca. 9.2	9.12 ± 0.02[b]	230 ± 2	0	0	0
	Run 3.2	Acetic acid: 0.08	6.2	150 ± 3	1000	1.9[c] 0.5 - 0.7[d]	178

a = Measured FFA content prior to the experiment. b = Determined via an ammonia dosing test. c = Velocity calculated with angular momentum of mixer and d = velocity using PIVlab. e = shear stress determined using PIVlab too [31].

2.4.5 Immersion and Re-immersion test procedure

Four coupons were used per immersion test (runs 1.1, 2.1 and 3.1). The PTFE liner was filled with ultrapure water. In run 2.1, the appropriate FFA stock solution was added to achieve the desired test solution chemistry. A sample was taken to measure pH and FFA concentration (run 2.1). The coupon holder containing the four coupons was placed into the filled PTFE liner and autoclaved, sealed, and sparged with nitrogen for 1 hour. After sparging, a 5.5 mL 0.025% ammonia solution was added to the autoclave via the high temperature, high pressure displacement pump in run 2.1 and 3.1. The 0.025% ammonia solution was made by injecting 0.25 mL of a 25% NH_4OH solution into 250 mL ultrapure water, which was sparged for 1 hour with nitrogen. The autoclave was pressurized to 20 bar using nitrogen, and heated to 230-250 °C. The system was left for 48 hours. Afterwards, a sample from the test solution was taken to measure pH and FFA concentration (run 2.1). Two out of four coupons were used for the oxide and coupon analysis, while the remaining coupons were used for the re-immersion corrosion tests (runs 1.2, 2.2, and 3.2). The obtained pH values of the Frist Condensate experiments served as input for the re-immersion tests. For the re-immersion tests, 0.1 v/v% acetic acid was dosed to the ultrapure water to achieve a pH of 6, which was verified. Similar to the immersion tests, the solution was sparged with nitrogen for 1 hour prior to pressurizing up to 20 bar with nitrogen. The autoclave was heated to 150°C and left for 48 hours with the stirrer set to 1000 rounds per minute (rpm).

Afterwards, a sample was taken to measure pH (and FFA concentration (run 2.2). The metal coupons were both used for oxide and coupon analysis.

2.4.6 Mass loss measurements

The mass loss was determined by weighing the specimen before and after the corrosion test when the chemical cleaning procedure had removed all corrosion products from the specimen with a minimum removal of the base material [32,33]. The average corrosion rate R (mm/y) was calculated using:

$$R = (K \times W)/(a \times t \times D) \quad \text{[Eq. 1]}$$

Where: K is a coefficient to calculate the corrosion rate in the desired units (8.76×10^4), W is the mass loss in g, to the nearest 0.1 mg, a is the surface area to nearest 0.01 (cm^2), t is the time of exposure to test solution in hours to nearest 0.1 h, and D is the density (g/cm^3, 7.85 g/cm^3 for carbon steel).

During chemical cleaning, the oxide layer was dissolved in a chemical solution of 5% w/w HCl, at a temperature of 50°C. A corrosion inhibitor, Lithsolvent 620, was added to this solution to minimize the removal of the pristine C1010 metal. Samples for dissolved iron measurements were taken at regular intervals of 3 to 5 minutes to monitor the oxide dissolution process. Coupons were removed from the chemical solution once dissolved iron contents remained stable, indicating all oxide had dissolved. After removing a coupon, it was flushed with ammonia water (pH 9-10) to temporarily passivate the material to avoid flash rusting.

The mass of the oxide layer ($M_{oxide\text{-}layer}$) was determined by subtracting the mass of the coupon determined after the chemical removal of the oxide layer from the mass of the coupon prior to this removal. The oxide layer thickness derived from the measured mass loss, called 'oxide thickness via weight loss' was determined via the following formula:

$$h_{oxide} \times 1 \times 10^{-4} = M_{oxide\text{-}layer} / (\rho_{oxide} \times A_{coupon}) \quad \text{[Eq. 2]}$$

Where: h_{oxide} is the thickness of the oxide layer (µm), $M_{oxide\text{-}layer}$ is the mass of the oxide (mg), A_{coupon} is the surface of the coupon (cm^2), and ρ_{oxide} is the density of magnetite (= 5000 mg/cm^3).

2.4.7 Surface analysis

The various surface analysis methods used to study the oxide surface layer formed during and present after the immersion, and re-immersion are X-ray diffraction (XRD), Scanning Electron Microscopy (SEM), and Energy Dispersive Spectroscopy (EDS) analysis. SEM images were taken of both the coupon/oxide surface and cross section.

The oxide layer thickness determined by SEM was used as an additional means to measure the corrosion rate via Eq. 1. This rate was called 'corrosion rate via SEM'. For this the loss in mass was,

among others, derived from the oxide volume and a chosen oxide density. The mass loss was determined via the following equation:

$$W = (M_{clean\text{-}coupon} - M_{coupon+oxide}) + (A_{coupon} \times (h_{oxide} /10000) \times \rho_{oxide}) \quad [Eq. 3]$$

Where W is the mass loss of the coupon over the immersion test (mg), $M_{clean\text{-}coupon}$ is the mass of the clean coupon prior to immersion. $M_{coupon+oxide}$ is the mass of the coupon including the oxide after the immersion test. A_{coupon} is the surface of the coupon (cm^2), h_{oxide} is the thickness of the oxide layer (µm) measured via SEM, and ρ_{oxide} is the density of magnetite (5000 mg/cm^3 [11,34]).

3 Results and discussion

3.1 Sampling campaign

3.1.1 pH and conductivity results and cycle chemistry guidelines

pH and conductivity are important parameters to monitor the cycle chemistry in steam-water systems. The measurement results from the ammonia plant cycle were compared with the IAPWS guideline [17] and the VGB guideline [18] to evaluate the operation status (Table 4). Although the two guidelines presented here were set for all-volatile treatment, the IAPWS guideline, for instance, is also recommended for pH control in a film-forming substance (including FFA)-treated system [3]. The measured pH values fit the IAPWS guideline very well, except for the value of the economizer inlet (P8) which was lower. However, this pH value stayed within the plant guideline, which is 8.8 – 9.2. When switching the traditional treatment program to the FFA-based method, it was attempted to control the pH of the economizer inlet above 9.2, in accordance with the IAPWS and VGB guidelines. However, it was not possible to reach this value. To avoid overdosing chemicals and to still maintain sufficient protection, the pH plant specification for the economizer inlet was set to 8.8 – 9.2 to maintain an alkalized environment, and a daily measurement of FFA in the boiler water was also required to be 0.01 – 0.2 mg/L to ensure enough FFA for film formation in the system. It is still less work to perform the daily FFA measurement than to monitor the on-line phosphate and sodium measurements in the previous treatment. To sum up, when adapting IAPWS and VGB guidelines to a certain plant, the local situation needs to be taken into account. If the guideline cannot be fully implemented, a combination of parameters is an option to ensure a safe operation.

The conductivity is suggested to be consistent with pH by the IAPWS guideline. The minimum conductivity was calculated based on the measured average pH (Table 4), which is the conductivity given by H^+, the protonated amines and OH^-. The conductivity of the economizer inlet (P8) and the low pressure (LP) drum blowdown (P11) were consistent with the measured pH. However, the result of the HP drum blowdown (P12) was below the calculated limit. The hypothesized cause was the slowly drifting response of the conductivity probe for low-conductivity samples. The online conductivity

measurement for HP drum blowdown (P12) showed a value of 3.9 µS/cm on average on the sampling day, which met the calculated minimum. This emphasized the importance of pH and conductivity measurement with good care for low conductivity samples.

Table 4. pH and conductivity measurement results with the IAPWS and VGB guidelines. The pH data: n=2, ± half difference; the conductivity data: n=3, ± standard deviation. ('/' meaning no specifications found)

Location	Sampling campaign			IAPWS guideline		VGB guideline
	pH	Conductivity measured (µS/cm)	Minimum conductivity calculated from pH (µS/cm)	pH	Conductivity (µS/cm)	pH
Economizer inlet (P8)	8.8 ± 0.2	1.5 ± 0.0	> 1.3	9.2 – 9.8	Consistent with pH	> 9.2
LP drum blowdown (P11)	9.4 ± 0.1	17.5 ± 0.0	> 5.0	9.0 – 9.8		/
HP drum blowdown (P12)	9.2 ± 0.2	2.7 ± 0.0	> 3.1	9.0 – 9.8		/

3.1.2 Resin compounds in the HP steam drum blowdown

An LC—HRMS method was developed for targeted analysis of OLDA and non-targeted analysis of organic compounds including potential degradation products of the dosed FFAP in the system [28]. Features (combinations of mass-to-charge ratio and retention time associated with a signal intensity) were obtained and were prioritized through the four following steps, (i) retention time cut-off, (ii) background removal, (iii) FFAP peaks removal and (iv) further selection based on peak shape and distribution profile among sampling points. Finally, this prioritization workflow resulted in features originating from the system with specific distribution profiles.

One FFAP degradation product and five potential degradation products were identified and prioritized in the reverse phase (RP) positive ionization results [28]. In the RP negative ionization results, six features were prioritized in the end, among which one feature was present in both LP and HP blowdown streams and the other five features showed high responses only in HP steam drum blowdown (P12). Next, mass spectrometry full scan (MS1) and tandem mass spectrometry (MS2) results were used to determine the chemical formula and structure of the features. The chemical formula of the six found features all contained one sulfur atom and three oxygen atoms (table in Figure 4), similar to the functional group in the cation exchange resin. In CPU1-3 (Figure 1), the turbine condensate, process condensate and demineralized water are treated by mixed bed resins to remove impurities. The cation exchange resin in these mixed beds has cross-linked polystyrene as matrix with a functional group of sulfonic acid ($R-S(=O)_2-OH$). In the first months after switching to the FFAP treatment (2013), the resin carried over from the mixed bed in CPU1 and entered the system. These

prioritized features were therefore suspected to originate from these resin beads. The MS2 spectra of the six features were uploaded to MetFrag Web beta (https://msbi.ipb-halle.de/MetFragBeta/) and mzCloud (https://www.mzcloud.org/) to retrieve candidates from the online databases. The suggested structures were evaluated based on similarities to the matrix and functional group in the resin. The top candidates of these six features all contained a benzene ring and a sulfonic acid functional group (Figure 4). The repeated fragments in multiple MS2 spectra corroborated these similar structures, which are displayed in Figure 4. To further confirm the suggested structures, the MS2 spectra records of feature A and B were obtained from online mass spectral databases. The spectral similarities between the analytical results of plant samples and the online records were calculated. For feature A, the similarity score (between 0, no similarity to 1, full accordance) was 0.98, based on the same major peaks and highly resembled relative intensities. For feature B, the similarity score was 0.76. However, the two spectra showed the same major peaks as well. There were relatively higher precursor peak and lower fragment peaks in the record spectrum compared to the plant sample spectrum. This was hypothesized to be due to the different collision energies on the same compound. According to all the results above, it was proven that features A-F were highly likely corresponding to the probable structures in Figure 4, thus most probably are compounds originating from the cation exchange resin.

The distribution of these resin compounds showed that they were mainly found in the HP steam drum blowdown (feature F also in LP steam drum blowdown). It indicated that resin beads were carried over in the drums after entering the steam-water system, where they decomposed over time. Since the carried over resin beads did not cause issues in the plant operation and the blowdown streams are discharged from the system regularly, these resin compounds were considered to have a negligible effect on the system.

Although there were no issues observed after the resin carryover incident, it still spotlighted the concern for the intrusion of contaminants. Since the lifetime of these contaminants can be long in the steam-water system, the developed non-target analysis of organic compounds helps to monitor the distribution of the contaminants and to predict the effects on the major units.

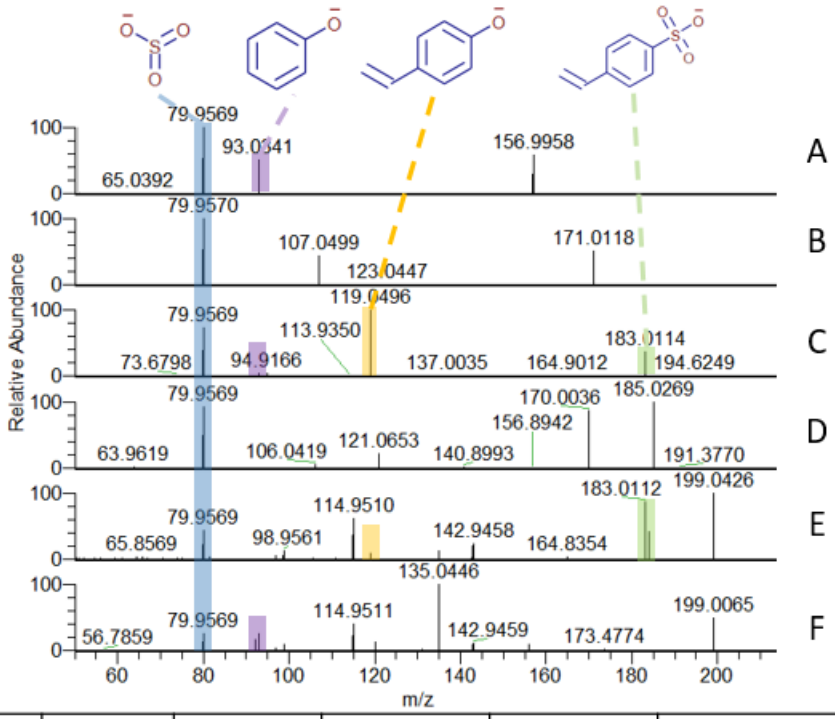

Features	A	B	C	D	E	F
Formula	$C_6H_6O_3S$	$C_7H_8O_3S$	$C_8H_8O_3S$	$C_8H_{10}O_3S$	$C_9H_{12}O_3S$	$C_8H_8O_4S$
Probable structures	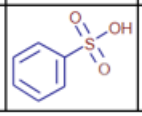	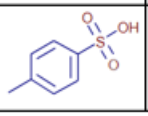	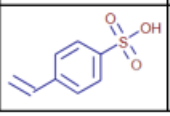	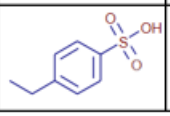	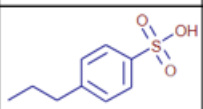	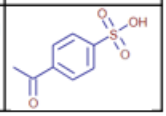

Figure 4. MS2 spectra of the prioritized six features with formula and proposed structures (A-F) in the table. Four fragments appeared in multiple spectra are annotated.

3.1.3 Plant inspection

Since the start-up with the FFAP treatment (2013), several of the HP steam system units have been internally inspected due to the government regulation and to ensure the integrity of the system. The inspection was mainly focused on the degasser, HP steamdrum and HP turbine. No corrosion related failures were found in this HP steam system till now. Only one FAC failure was observed in the HP blowdown line in 2019, caused by a leaking blowdown valve. In the production site, the injection of this HP steam with FFAP was not affecting the process catalyst [27]. The effect on heat transfer efficiency due to FFAP treatment cannot be measured due to the complexity of the steam system. Yet the positive effects of the treatment could be also seen with the blowdown frequencies. The amount of the LP and HP steamdrum blowdown is almost reduced to zero, achieving less water consumption and energy loss.

3.2 Methanol lab-scale boiler experiments

Methanol is a main TOC contributor in this steam-water system [16]. The degradation at different pH values was investigated with the lab-scale boiler system (Figure 5) under the HP steam system conditions. In experiment 1, the pH of the 13 mg/L methanol solution in MilliQ water was 5.6, most probably due to the intrusion of CO_2 from the air. In both experiments, the average methanol

concentrations were lower in the condensate samples than in the feed samples. However, a t-test only proved a significant 6% difference in methanol concentration between the feed and condensate in experiment 2. The methanol decrease in experiment 1 was not proven to be significant due to the high variance of the condensate results. In experiment 2, formate was analyzed by ion chromatography in the feed and condensate samples. However, the concentrations were below the quantification limit of the method for formate (0.13 mg/L). It was not possible to confirm if formate was generated from the methanol degradation.

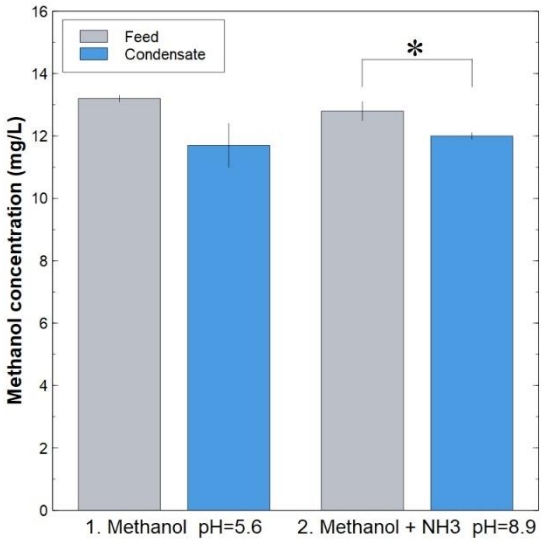

Figure 5. Methanol results (mean) in the lab-scale boiler experiments with error bars expressed as standard deviation (n=3). * indicates statistical significance.

3.3 First condensate (FC) experiments

3.3.1 Set-up conditions

Preliminary trials with ultrapure water were conducted with the first condensate set-up to derive the optimal conditions and to obtain unsaturated steam with a steam quality of 90%. This is the relative mass fraction of liquid water in the vapor phase [29]. A flowrate of 12 mL/min and a FSB temperature of 250°C were set to obtain these requirements. It was seen that both the temperature and the pressure inside the system gradually increased and stabilized at respectively 180°C and 10 bar, reaching a steam quality of 90%, *i.e.* 10.8 mL/min bulk condensate (BC) was collected at the end, meaning that 1.2 mL/min was collected in the first condensate chamber. However, both temperature and pressure slightly decreased when collecting the first condensate, decreasing the flowrate of the bulk steam to 6 mL/min. It took on average 5 minutes to restore the bulk steam flow rate to 10.8 mL/min when 25 mL first condensate was collected. Therefore, average steam quality was lower than predetermined (60-74%).

3.3.2 pH change in first condensate

Figure 6 summarizes the experimental and model derived pH values from both the ammonia (A) and ammonia-formate-acetate (A-F-A) experiments. In both experiments, a pH of around 6 is found in the FC, which is more acidic than the feed pH. On the other hand, there is no significant difference between feed and BC pH, meaning the formation of FC did not induce a change in the bulk pH. However, the feed pH of the A-F-A experiment is lower than expected for a 0.5 mg/L solution of both ammonia, formate and acetate (+/- 8.7). Feed samples were taken regularly during the experiment and it was seen that a homogeneous concentration of 0.5 mg/L ammonia was only reached near the end of the experiment, while formate and acetate were found directly at 0.5 mg/L from the start of the experiment. This explains the lower pH in practice and this was taken into account for the model calculations.

The pH values of FC obtained in both experiments match very well with the pH values generated by the model. Both for the model and experiment, the pH of FC is 1.3-2.8 units lower than that of BC, and this for both conditions tested. Others observed a decrease of 0.5-1.5 units with real industrial steam [20,21]. The different results are probably explained by differences in the experimental setup and by the less complex composition of the simulated feed water used in lab scale. For example, the presence of other anionic contaminants and cations can influence the FC pH [21].

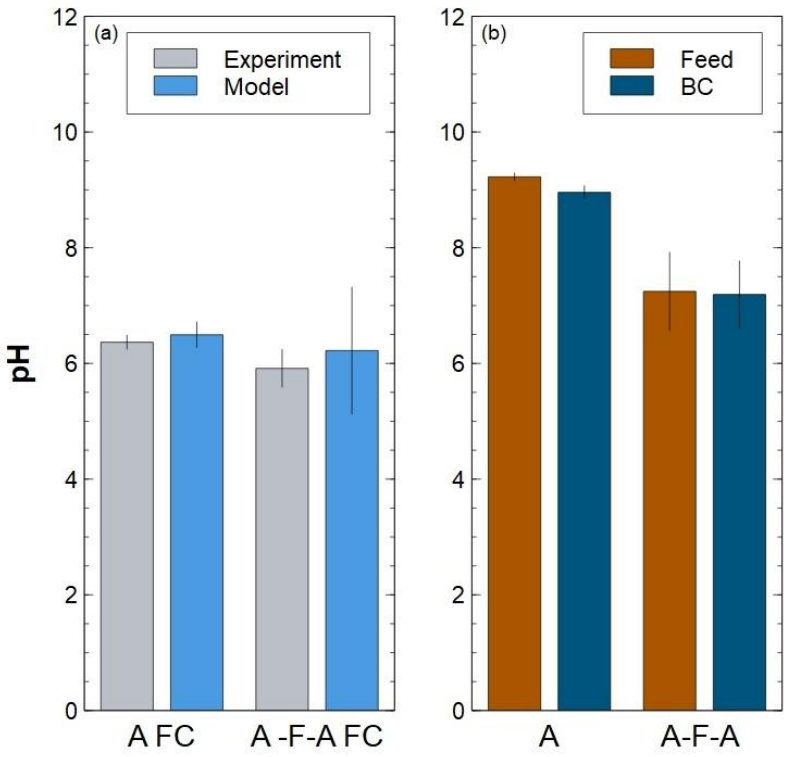

Figure 6: pH values of feed, first condensate (FC) and bulk condensate (BC) with CO_2 dissolution included, (a) pH of FC obtained empirically (grey) and estimated by the model (light blue), (b) pH of feed (brown) and BC (dark blue). A = ammonia experiment, A-F-A = ammonia-formate-acetate experiment. Empirical standard deviations

were obtained by 5-6 different sample rounds. Steam quality and ammonia feed concentration changed in every sample round and therefore, 5-6 different pH calculations were done with the model.

The pH of FC and BC did not change significantly when adding formate and acetate to the feed. This phenomenon can be clarified by the relative volatility (= concentration in BC/concentration in FC) which is calculated from the ion chromatography results from each sample round (Figure 7). The mean relative volatility of formate and acetate was 0.32 and 0.13, meaning that the concentration in FC is 3-10 times higher than in BC. On the other hand, when formate and acetate are present in the steam, the relative volatility of ammonia drops from 1.8 to 1.0. The concentration of ammonia in the FC in the latter scenario will thus be higher and will act as a buffer in the FC, explaining the negligible pH change between the two experiments. This trend is also seen by the model, although the relative volatility values calculated differ from the ones obtained empirically and need further investigation.

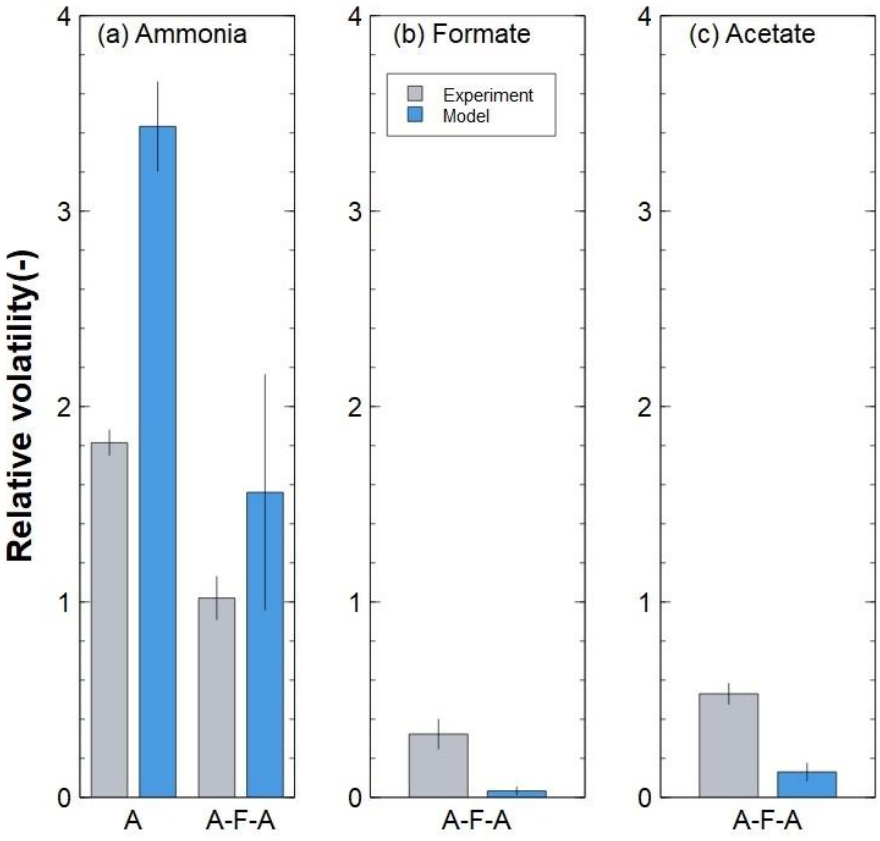

Figure 7: Relative volatility of (a) ammonia, (b) formate and (c) acetate both empirically (grey) and estimated by the model (blue). A = ammonia experiment, A-F-A = ammonia-formate-acetate experiment. Empirical standard deviations were obtained by 5-6 different sample rounds. Steam quality and ammonia feed concentration changed in every sample round and therefore, 5-6 different relative volatility calculations were done with the model.

These results imply that a lower pH can occur in the first condensate in SWC, even if the pH of the bulk condensate is still in agreement with the plant guidelines. However, in this research, the presence of acids in the steam improve ammonia condensation (relative volatility = 1) to the first condensate and

thereby partially buffering the pH. Nonetheless, the concentrations of acetate and formate used in this study are approximately 10 times higher than what is generally found in SWC [15]. Also, in the SWC of concern alkalizing amines, i.e. ethanolamine and cyclohexylamine, instead of ammonia, are used for pH control. Ethanolamine is less volatile than ammonia and might better control the pH in the first condensate [35]. The model and the lab-scale set-up can be used in the future to predict the first condensate pH of more complex steam compositions and as such, to have a more precise idea of the pH in the first condensate in real steam-water systems.

3.4 Corrosion tests

3.4.1 Effect of FFA on oxide layer thickness

The oxide layer thickness determined via the SEM images is presented together with the oxide layer thickness determined via the weight loss measurements in Figure 8.

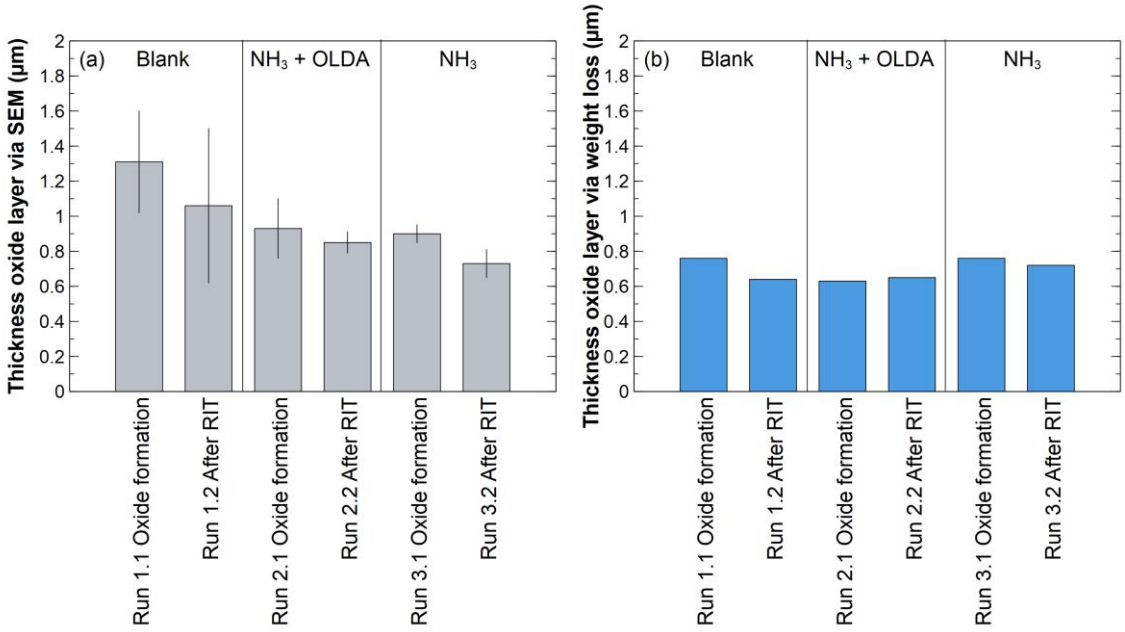

Figure 8: Oxide layer thickness via (a) SEM and (b) weight loss, after the immersion test (oxide formation) and re-immersion test (RIT). (a) standard deviation from the measurements at various locations of the cross-section, (b) no standard deviation as one coupon was used per weight loss measurement.

The oxide layer formed under the untreated medium (blank) chemistry was much thicker when determined via SEM. This notable difference between Figure 8a and b can be related to the nature of the two measurements. The SEM image was taken at the cross-section at the "point of impact", directly facing the mixer, whereas the weight loss was determined over the entire coupon. PIVLab [31] derived hydrodynamics showed the highest flow rates to be near the mixer, and SEM surface images at points other than the impact point showed less erosion of magnetite crystals after the re-immersion test. Moreover, a fixed magnetite density was assumed to calculate the oxide thickness from the weight loss data, whereas literature reports denser magnetite layers after the addition of FFA [5,36,37]. This

means that the oxide layer formed under a blank chemistry could indeed be less dense compared to the other layers, and therefore the density used to calculate the layer thickness from the weight loss data was not representative. A density of 2.9 g/cm^3 would have yielded a similar thickness for the oxide layer formed under a blank chemistry, run 1.1. This could not be directly verified from the SEM cross section images, as the resolution was not sufficient to see any pores.

Figure 8a clearly shows the oxide layer which was formed under untreated medium (blank), formed the thickest oxide layer. Figure 8a and b both show a similar trend on how the oxide layer thicknesses before and after the re-immersion tests relate to each other. Figure 8a shows the strongest reduction during the re-immersion test for the layers formed in the blank, and NH_3 conditions. The reduction in thickness, between formation and after the re-immersion test, found for SEM are 19.1%, , 8.6% and 23.3% for blank, OLDA + NH_3, and NH_3 respectively. Figure 8b shows the strongest reduction for the layers formed under blank, and NH_3 only conditions as well, and even a slight increase for the layers formed under OLDA addition. The reduction (indicated with a minus sign) or increase in thickness are -15.8%, 3.2% and -5.3% for blank, OLDA + NH_3 and NH_3.

According to the SEM and weight loss determined oxide thickness, the layers produced under FFA addition were reduced less under re-immersion conditions. Furthermore, looking at Figure 8a, it seems that FFA slowed the formation of an oxide layer. However, the layer formed during the blank immersion test was the only layer formed at 250 °C, instead of 230 °C. It is known that the Schikorr reaction is more rapid at higher temperatures. Dubey and Kain [38] report larger magnetite grains formed at higher temperatures under similar conditions.

3.4.2 Effect of FFA on oxide layer formation

The SEM cross sections images from which the "SEM derived surface thicknesses" were determined are depicted in Figure 9. These SEM images were taken after the immersion experiments testing, the blank (untreated) chemistry, OLDA and NH_3 chemistry and NH_3 chemistry. The presence of an oxide layer was confirmed using EDS.

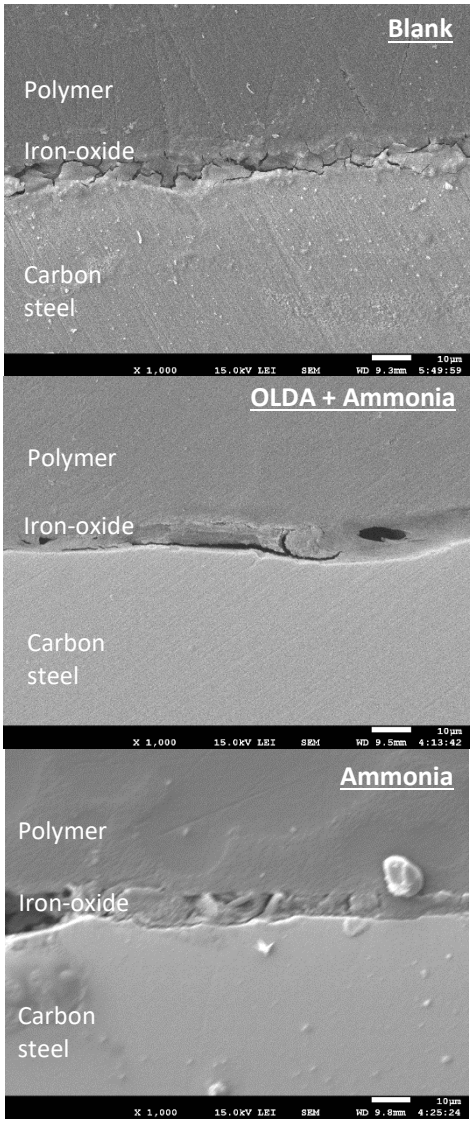

Figure 9. SEM cross section images taken after the immersion test, depicting the iron-oxide layer (middle, white), carbon steel (below) and polymer embedding material (above, dark grey).

Figure 9 shows the effect of the different treatment methods on the homogeneity and "smoothness" of oxide surface layer. In all cases of an immersion test with an additive showed a smooth and thin layer. Smoother layers were visually observed for runs with OLDA present. It also appears that layers formed under OLDA are the most homogeneous. This is in accordance to what is published in literature [6,7,36,37].

3.4.3 Effect of FFA on corrosion rate

Figure 10a shows the corrosion rate determined via the SEM measured oxide thickness and Figure 10b presents the corrosion rate determined via weight loss. Corrosion rates were determined over the immersion test run, given as X.1, and over both immersion and re-immersion test runs combined, given as X.2. referred to as the "overall corrosion rate".

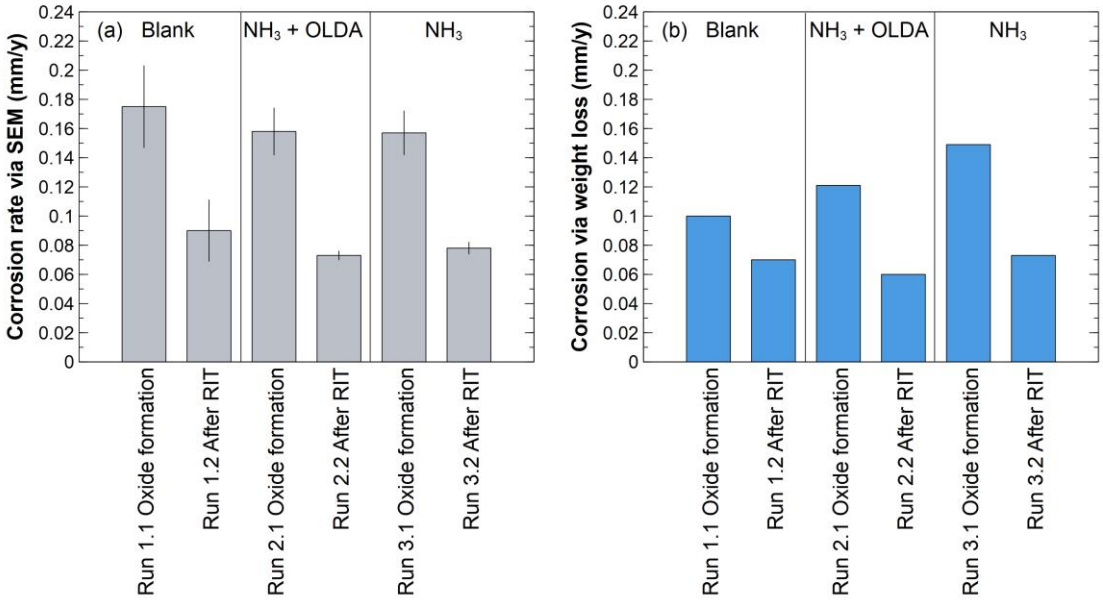

Figure 10: Corrosion rates determined after the immersion tests (oxide formation), and overall corrosion rates determined after the re-immersion tests (RIT) via (a) SEM images and (b) weight loss measurements.

Both Figure 10a and 10b show a similar trend where the overall corrosion rates were only 50% of the corrosion rates determined after the immersion test. The layer formed under OLDA shows the most reduction in corrosion rate and had the lowest overall corrosion rate measured after the re-immersion run. The efficiency of the corrosion inhibition was calculated, this was done based on the corrosion (rates) via weight loss. The inhibition values compared to the blank were 14.3% for OLDA in addition to NH_3, and no inhibition under the NH_3 only chemistry.

The Schikorr reaction is an autonomous process that cannot be halted. After a magnetite layer has formed, it offers protection against any further corrosion, as the overall corrosion rate measured half the value of the corrosion rates determined after the immersion tests. This was not the case for the blank chemistry. Having a lower corrosion rate during the first run and a relatively high one after the re-immersion test, 0.07 mm/y. The low rate could be influenced by the higher temperature of 250°C applied during the test, opposed to 230°C.

FAC (flow accelerated corrosion) is very relevant and important for high end water steam cycles and literature suggests the positive effects of using FFA and their products for FAC. [8] The dynamic re-immersion tests performed in this study can be considered as simplified conditions imitating FAC conditions. Even though similar acidic conditions were simulated, this study found 50 times lower corrosion rates than what was reported by Weerakul *et al.* [8], which are 2.84 to 8.69 mm/y for a blank chemistry at 140°C. The higher rates can be a result of higher fluid velocities and shear stress, 13.06 m/s and 388 Pa compared with 1.9 m/s and 178 mPa in this study. It should be noted that the

shear stress was determined via PIVlab, which calculated a range of velocities based on videos of the setup. It could therefore be underestimated in this study. Another difference between the two work is the chromium content, as Lister and Uchida [39] report on the linear dependence of FAC rate on chromium content. The carbon steel used in the literature [8] and this work contain 0.001 wt% and 0.0580 wt% chromium, respectively.

3.4.4 XRD and Contact angle analysis

XRD analyses were performed on the lower part of the coupon. In case of the re-immersion experiments the location of XRD analysis was at the coupon side facing the mixer. All XRD results indicated the presence of metallic iron and magnetite. No other compounds were detected. Evidently the presence of OLDA did not suppress the oxide layer formation.

3.4.5 SEM surface images

Figure 11 shows the representative SEM surface images taken from the oxide surface after the immersion and re-immersion tests. Figure 11a, c and e, show the oxide surface after the immersion test. Under the blank, and ammonia only solutions, a fully grown secondary layer can be seen composed of visible magnetite crystals, showing cubic, octahedral faces, with sharp corners and edges. The layer formed under the blank conditions had the biggest crystals, and the layer formed under ammonia had smaller, not fully grown crystals. Concerning the secondary magnetite layer formed under the OLDA and ammonia chemistry, except for some areas, (see Figure 11c) no uniform growth of magnetite crystals was identified.

The SEM images of Figure 11 do support the notion that under higher temperatures magnetite crystals grow faster. The argument given is that the layer formed under a blank chemistry was the only test performed at 250 °C. However to conclude upon this would be premature as this was also the only test with a neutral pH value. Moreover, the SEM surface images do also support the notion that the blank formed layer was less smooth compared to the layers formed under the other chemistries.

Figure 11b, d and f, show the oxide surface after the re-immersion test. The SEM surface image b shows far smaller, sharper, to no magnetite crystals, indicating heavy dissolution and erosion of the magnetite layer formed under a blank chemistry during the re-immersion test. This dissolution and erosion effect was also observed for the other layers. SEM surface image f shows better grown crystals as compared with image e, however not uniformly covering the surface.

Under the OLDA treatment no uniform secondary magnetite layer was formed. It could be that the OLDA film covered the coupon, leading to crystals only growing at microstructural irregularities. To verify this in future research, one should accurately identify these growth locations and observe them again, after cleaning the oxide using SEM. Another option to explain the irregular magnetite crystals

found on the surface could be magnetite colloid deposition. Although, the magnetite crystals were more likely to have formed at the surface comparing to the SEM images of Gasnier and Lister [40], showing an image of deposited magnetite colloids, looking more floc like, dispersed, and loosely attached to the surface.

Even though the conditions cannot be attributed to FAC as mentioned before, some similarities were still found with the previous research. Kain *et al.* (2014) [46] mentioned scallops as a typical pattern. In our study, such structures were not observed under SEM or optical microscope. However, the study of Weerekul *et al.* (2020) [12] reported no scallops but corroded surface as `ragged and porous` instead, which is more similar to what was observed in this study (Figure 11b).

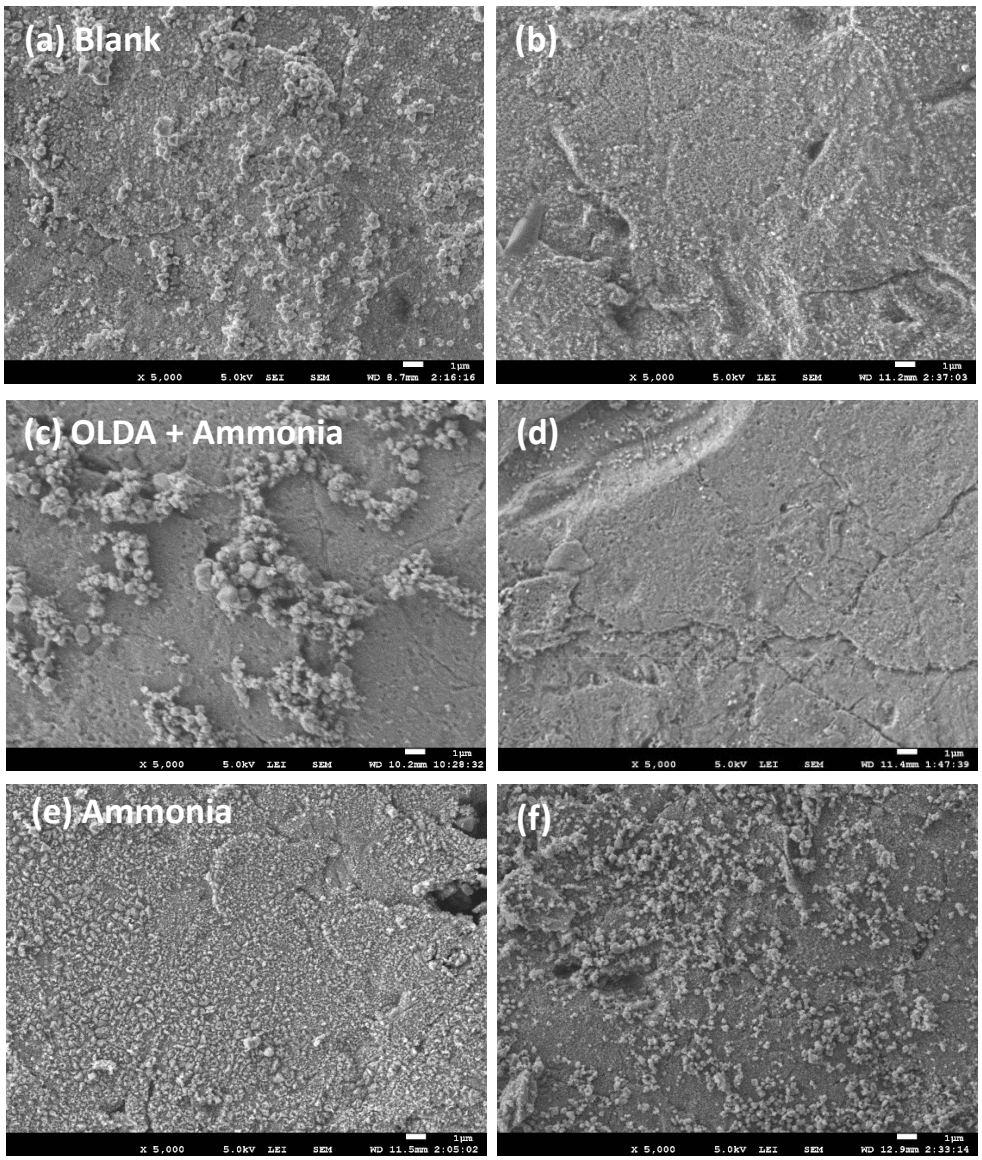

Figure 11. Surface morphologies of carbon steel samples after exposure to immersion tests (a) blank solution (c) OLDA and ammonia solution and (e) ammonia solution. The surface morphologies of b, d and f are the respective re-immersion tests under acidic (pH of 6) conditions, combining a and b, c and d, e and f as immersion and subsequent re-immersion tests. Magnifications 5000x.

4 Conclusion

The distribution of organic compounds and the parameters, including pH and conductivity, in the FFAP-treated steam-water system of an ammonia production plant were studied with the results from a sampling campaign. The water and steam parameters were in accordance with IAPWS and VGB guidelines with some modifications based on the local situation. There were no issues observed in the plant after the resin carryover incident and the six resin compounds were mainly found in the HP blowdown stream, which is discharged from the system regularly. The effect of these resin compounds was considered to be negligible on the steam-water system. The stability tests of methanol, the main TOC contributor in the system, showed that the methanol degradation occurred under the alkalized HP steam system condition.

Preliminary lab-scale experiments with an ammonia or ammonia-formate-acetate containing simulated feed water clearly showed the drop in pH in the first condensate compared with the bulk stream. On the other hand, the relative volatility of ammonia decreases in the presence of acids, buffering the pH of the first condensate. A model can predict the pH in this first condensate very well and should be optimized with other compounds to have a better simulation of real steam-water cycles. This will allow a better estimation on the corrosion potential of first condensate droplets.

The immersion tests indicated a sufficient growth of oxide layers on C1010 metal coupons. X-Ray diffraction measurements indicated that under all chemistries, magnetite was formed as the only compound. SEM and EDS cross section images showed that for all additives, thinner layers were formed than under a blank chemistry. Combined with SEM images, it was observed that OLDA in addition to ammonia formed magnetite layers of similar thickness to those under ammonia only chemistry, but being smoother and more uniform.

During the re-immersion tests, acidic condition was applied along with a stirred setup and an acetic acid chemistry with pH of the obtained first condensate. The magnetite layers formed under OLDA added to ammonia were more resistant under acidic conditions than the layers formed under the ammonia only chemistry, and blank chemistry, with less reduction of the magnetite layer thickness. SEM surface images showed the magnetite crystals formed under the blank chemistry were affected by dissolution and erosion the most. The layer formed under OLDA had the lowest overall corrosion rate measured after the re-immersion test.

After 8 years of FFAP treatment in this HP steam system, no corrosion failures occurred. No incidents due to high oxide deposits on the high heat transfer waste heat boiler tubes were observed. In combination with the results of the lab studies, it confirms that the FFAP is a safe treatment of a steam-

water cycle even in case where significant amounts of contaminant by organic matter, in this case methanol, is present.

5 Outlook

- Adjustments and probably extra requirements are needed when adapting an universal guideline to a plant. Contaminants may stay years after their introduction to the steam-water system. The developed LC-HRMS non-target analysis method helps to monitor the distribution of (specific) organic compounds and to predict the potential effects.
- Improvement of the first condensate set-up is needed to reach the targeted steam quality (90%). Thereafter, alkalizing amines and other organic contaminants in the steam-water cycle should be included in the lab-scale experiment to assess the composition in the first condensate and the potential corrosion risk.
- Additional corrosion experiments are needed to increase the statistical power, thereby confirming a lower corrosion rate with the OLDA treatment. Besides the tests conducted here, more realistic tests under single-phase or two-phase FAC would be useful to demonstrate the lower corrosion rates when using OLDA. This is beneficial for the condensate systems and complex boiler systems where an accumulation of acid/breakdown products can occur.

6 Acknowledgement

This work was financially supported by “Steam and Condensate Quality Water Process Technology” project under the framework of Institute for Sustainable Process Technology. The project is co-funded with subsidy from the Topsector Energie by the Ministry of Economic Affairs and Climate Policy.

The authors would like to thank Durga Mainali for preparing samples for SEM and taking SEM photographs. The authors would like to recognize Sonja Vidojkovic’s help in setting up the magnetite setup. The authors would also like to thank Samuel Bodé for his valuable inputs in adjusting the first condensate setup. Ruud Hendrikx at the Department of Materials Science and Engineering of the Delft University of Technology is acknowledged for the X-ray analysis.

7 Reference

[1] D. Einstein, E. Worrell, M. Khrushch, Steam systems in industry: Energy use and energy efficiency improvement potentials, 2001. https://escholarship.org/uc/item/3m1781f1%0A.

[2] V.J. Linnenbom, The Reaction Between Iron and Water in the Absence of Oxygen, J. Electrochem. Soc. 105 (1958) 322–324.

[3] Technical Guidance Document: Application of Film Forming Substances in Industrial Steam Generators, IAPWS TGD11-19, 2019. http://www.iapws.org/techguide/FFS-Industrial.pdf.

[4] Technical Guidance Document: (2019 Revision) Application of Film Forming Substances in Fossil, Combined Cycle, and Biomass Power Plants, IAPWS TGD8-16, 2019. http://www.iapws.org/techguide/FFS.pdf.

[5] P. Janssen, J. Savelkoul, In search of an alternative high-pressure boiler water treatment

program, PowerPlant Chem. 14 (2012) 440–448.

[6] H. Topp, W. Hater, A. de Bache, C. zum Kolk, Film-forming amines in shell boilers, PowerPlant Chem. 14 (2012) 38–48.

[7] H. Topp, D. Steinbrecht, W. Hater, B. Giulini, A. de Bache, The influence of film-forming amines on heat transfer during saturated pool boiling, PowerPlant Chem. 12 (2010) 388–395.

[8] S. Weerakul, N. Leaukosol, D.H. Lister, S. Mori, W. Hater, Effects on flow-accelerated corrosion of oleylpropanediamine under single-phase water conditions pertinent to power plant feedwater, Corrosion. 76 (2020) 217–230. https://doi.org/10.5006/3225.

[9] R. Bäßler, M. Uhlemann, K. Mummert, Inhibiting effect of octadecylamine on pitting corrosion behaviour of stainless steel type 1.4541 up to 250 °C, Mater. Corros. 50 (1999) 146–153. https://doi.org/10.1002/(sici)1521-4176(199903)50:3<146::aid-maco146>3.0.co;2-g.

[10] E.V. Chernyshev, E.N. Veprov, V.A. Petrov, S.L. Bogdanov, T.Y. Levina, T.I. Petrova, V.I. Kashinskii, A.A. Zonov, A.E. Verkhovskii, Increasing the corrosion resistance of equipment due to the use of film-forming amines, Power Technol. Eng. 40 (2006) 34–37.

[11] E. Jäppinen, T. Ikäläinen, S. Järvimäki, T. Saario, K. Sipilä, M. Bojinov, Corrosion Behavior of Carbon Steel Coated with Octadecylamine in the Secondary Circuit of a Pressurized Water Reactor, J. Mater. Eng. Perform. 26 (2017) 6037–6046. https://doi.org/10.1007/s11665-017-3035-6.

[12] S. Odar, Use of film forming amines (FFA) in nuclear power plants for lay-up and power operation, ANT Int. (2017). https://antinternational.com/handbooks-and-reports/use-of-film-forming-amines-ffa-in-nuclear-power-plants-for-lay-up-and-power-operation/.

[13] D.H. Moed, A.R.D. Verliefde, L.C. Rietveld, Effects of Temperature and Pressure on the Thermolysis of Morpholine, Ethanolamine, Cyclohexylamine, Dimethylamine, and 3-Methoxypropylamine in Superheated Steam, Ind. Eng. Chem. Res. 54 (2015) 2606–2612. https://doi.org/10.1021/ie504849v.

[14] A. Söllner, W. Glück, K. Höllger, W. Hater, A. de Bache, Comparison of Four Steam Generators Regarding the Decomposition Products of Amines, VGB PowerTech 3. (2013) 61–66.

[15] B. Kolander, A. de Bache, W. Hater, Experience with Treating the Water/Steam Cycle in the Nehlsen Stavenhagen RDF Power Plant with Film-Forming Amines, PowerPlant Chem. 15 (2013) 137–145.

[16] J. Savelkoul, R. Van Lier, Operational Experience with Organics in Industrial Steam Generation, PowerPlant Chem. 7 (2005) 733–739.

[17] Technical Guidance Document – 2015 Revision: Volatile treatments for the steam-water circuits of fossil and combined cycle/HRSG power plants, 2015. http://www.iapws.org/techguide/Volatile.html.

[18] VGB-Standard Feed Water, Boiler Water and Steam Quality for Power Plants/Industrial Plants, VGB PowerTech, Essen, Germany, 2011. VGB-S-010-T-00;2011-12.EN.

[19] E. De Meyer, The behavior of organic matter in industrial demineralization and steam-water cycles, Ghent University, 2020.

[20] J. Savelkoul, P. Janssen, H. Verhoef, Monitoring of First Condensate Corrosion (FCC) in Industrial Steam Systems, PowerPlant Chem. 3 (2001) 326–330.

[21] R. Svoboda, H.-D. Pflug, T. Warnecke, Investigation into the Composition of the Early

Condensate in Steam Turbines, PowerPlant Chem. 5 (2003) 273–280.

[22] M. De Wispelaere, Early Condensate in a Fossil Power Plant using organic treatment, 14th Int. Conf. Prop. Water Steam Kyoto. (2004) 602–605. https://www.sciencedirect.com/science/article/pii/S0266353803001787.

[23] Steam and Condensate Quality Project, (n.d.). https://ispt.eu/projects/condensate-quality/ (accessed October 13, 2021).

[24] Institute for Sustainable Process Technology, (n.d.). https://ispt.eu/ (accessed October 13, 2021).

[25] I. Veleva, M. Vanoppen, I. Hitsov, R. Phukan, L. Wyseure, K. Dejaeger, E.R. Cornelissen, A.R.D. Verliefde, Selection of membranes and operational parameters aiming for the highest rejection of petrochemical pollutants via membrane distillation, Sep. Purif. Technol. 259 (2021) 118143. https://doi.org/10.1016/j.seppur.2020.118143.

[26] I. Veleva, W. Van Weert, N. Van Belzen, E. Cornelissen, A. Verliefde, M. Vanoppen, Petrochemical condensate treatment by membrane aerated biofilm reactors: A pilot study, Chem. Eng. J. 428 (2022) 131013. https://doi.org/10.1016/j.cej.2021.131013.

[27] F. Raeymaekers, Polyamine treatment in HP steam system of an ammonia plant, in: 62nd Annu. Saf. Ammon. Plants Relat. Facil. Symp., New York, USA, 2017: pp. 113–124.

[28] Y. Xue, D. Vughs, W. Hater, H. Huiting, M. Vanoppen, E. Cornelissen, A. Verliefde, A.M. Brunner, Liquid chromatography-high-resolution mass spectrometry-based target and nontarget screening methods to characterize film- forming amine-treated steam-water systems, Ind. Eng. Chem. Res. 59 (2020) 22301–22309. https://doi.org/10.1021/acs.iecr.0c05051.

[29] D.H. Moed, Organic Contaminants and Treatment Chemicals in Steam-Water Cycles, Delft University of Technology, 2015.

[30] A. Graf, Method for the determination of polyamines. https://patents.google.com/patent/EP0562210A1/en.

[31] W. Thielicke, E.J. Stamhuis, PIVlab – Towards User-friendly, Affordable and Accurate Digital Particle Image Velocimetry in MATLAB, J. Open Res. Softw. 2 (2014). https://doi.org/10.5334/jors.bl.

[32] ASTM G31-21, Standard guide for laboratory immersion corrosion testing of metals, ASTM Int. West Conshohocken, PA. (2021). www.astm.org.

[33] ASTM D2688-15e1, Standard Test Method for Corrosivity of Water in the Absence of Heat Transfer (Weight Loss Method), ASTM Int. West Conshohocken, PA. (2015). www.astm.org.

[34] J.S. Laskowski, Surface chemistry fundamentals in fine coal processing, in: Coal Handb. Towar. Clean. Prod., Elsevier, 2013: pp. 347–421. https://doi.org/DOI: 10.1533/9780857097309.2.347.

[35] J.A. Mathews, EPRI Assessment of Amines in Power Plant Chemistry Applications, PowerPlant Chem. 14 (2012) 268–274.

[36] W. Hater, A. de Bache, Film-forming amines in boiler feed water treatment, IPW (Int. Pap. World). (2010) 10–11.

[37] W. Hater, J. Jasper, P. Kraft, The film formation and corrosion inhibition of oleylamines on aluminium, in: Proc. EUROCORR 2021, Pap. No.52327, Montpellier, 2021.

[38] V. Dubey, V. Kain, Oxidation Behavior of Carbon Steel: Effect of Formation Temperature and pH of the Environment, J. Mater. Eng. Perform. 26 (2017) 5312–5322. https://doi.org/10.1007/s11665-017-3027-6.

[39] D.H. Lister, S. Uchida, Reflections on FAC mechanisms, PowerPlant Chem. 12 (2010) 590–597.

[40] C. Gasnier, D.H. Lister, The Effects of Chemical Additives on Magnetite Deposition in Boiling Heat Transfer, in: Int. Conf. Heat Exch. Fouling Clean., 2013: pp. 85–93.